scientific reports

Check for updates

OPEN

Exploration of the reactivities of homemade binary pyrotechnics

Chengbo Ru[1,2,3], Lihong Chen[1,2,3], Hongguo Zhang[1,2,3], Hongxing Wang[4], Hailong Xu[3,5], Zhiwei Chi[6] & Yanchun Zhang[1,2]✉

Understanding the properties of explosives is the basis for investigating and analyzing explosion cases. To date, due to the strict legal control of standard explosives and initiators, homemade pyrotechnics composed of oxidizers and fuels have become popular explosive sources of improvised explosive devices (IEDs) threatening greatly social stability and personal safety. The reactivity of pyrotechnics strongly depends on their intrinsic characteristics and operating conditions, which determine the efficiencies of heat and mass transfer between the reaction zone and the unreacted zone. Herein, the tests of thermodynamics, pressurization characteristics, and combustion propagation behaviors are conducted to explore the effects of oxidizer species, particle size, and loading density on the reactivity of homemade binary aluminum-based pyrotechnics. The results show that the pyrotechnics with potassium chlorate ($KClO_3$) have the strongest reactivity with the highest pressurization rate (dp/dt) and the shortest combustion duration. Compared with their counterparts based on aluminum microparticles(mAl), pyrotechnics consisting of Al nanoparticles (nAl) possess superior reactivity as expected, which results from the relatively short heat and mass transfer distances. The nAl-based pyrotechnics have a low reaction exothermic peak temperature, great heat release, great aluminothermic reaction completeness, and high produced peak pressure with several orders of magnitude higher pressurization rate. Increasing the loading density of the pyrotechnics over a certain value can change the dominant mode of heat transfer from convective to conduction, sharply decreasing the pressurization characteristics and combustion front propagation velocities (v_p). The results of theoretical calculations using the NASA-CEA codes show that loading density can alter the reaction process of the pyrotechnics, leading to a decrease in the predicted pressure per unit mass for Al/KNO_3 or Al/AP, and an increase for Al/$KClO_3$. For nAl/potassium nitrate (KNO_3), the density is between 1.0 and 1.25 g cm^{-3}, across which dp/dt decreases by one order of magnitude from 0.148 to 0.014 MPa ms^{-1}. In addition, v_p decreases by three orders of magnitude from 0.040 to 0.078 m s^{-1}. Distinct pressurization behaviors of nAl/AP are observed at a density of 1.5 g cm^{-3}, while the variation in nAl/$KClO_3$ reactivity fluctuates. These results are beneficial for the damage assessment of scenes caused by an explosion and for inversely calculating charge parameters.

Keywords Homemade pyrotechnics, Improvised explosive devices, Loading density, Pressurization characteristics, Combustion propagation

Improvised explosive devices (IEDs) composed of initiation systems, explosive materials, on-off control systems, and containers pose a great threat to social stability and personal safety. Due to the strict legal control of standard military and industrial explosives and initiators, pyrotechnics obtained from fireworks or crackers and their homemade counterparts become the main charge of the IEDs[1,2] employed in criminal and terrorist activities[3,4]. Pyrotechnics can be easily ignited by a fuse or an electrically heated wire, then react in a manner of combustion or deflagration, resulting in a blast. After an explosion occurs, scientific investigations and analyses of explosion scenes including device reconstruction, residue analysis, charge mass inverse calculation, explosive source track, and initiation mode evaluation, are necessary. Thereinto, the deduction of relevant information about the explosives from the trace features of objects damaged by a blast is vital. The intensity of the imprints

[1]College of Forensic Science, Criminal Investigation Police University of China, Shenyang 110854, China. [2]Key Laboratory of Impression Evidence Examination and Identification Technology, Ministry of Public Security, Shenyang 110854, China. [3]Key Laboratory of Liaoning Province Forensic Science, Shenyang 110854, China. [4]School of Energy and Water Resources, Shenyang Institute of Technology, Fushun 113122, China. [5]Shenyang Institute of Forensic Science, Shenyang 110000, China. [6]Ningbo Public Security Bureau, Ningbo 315048, China. ✉email: zhyanchun@163.com

resulting from an explosion is determined by the destructive strength of IEDs, which depends on the reaction characteristics of the explosives[5–8].

In terms of composition, pyrotechnics are composite energetic materials composed of oxidizers, reducers, and sometimes functional additives. Unlike those of monomolecular energetic materials, the reactivity of pyrotechnics directly depends on the efficiencies of heat transfer and mass transfer between the reacted zone and the unreacted zone, which is greatly affected by the species of ingredients, particle size, loading density, confinement strength, and initiation mode. Countless pyrotechnics exist because of the variety of oxidizers (nitrate, chlorate, perchlorate, metal oxides, iodate, permanganate, and other compounds with oxidizing ability) and fuel (aluminum, magnesium, aluminum magnesium alloy, titanium, sulfur, phosphorus, and charcoal) that can be randomly assorted, accordingly, their reactivities vary considerably. Skull model experiments conducted by Zwirner[9] revealed that 2.0 g of flash powder ($Al/KClO_4$) can lead to severe skull fractures, while 2.0 g of black powder does not cause bone fractures. The levels of blast overpressure produced by four brands of consumer crackers and one brand of consumer bottle rockets exhibit distinct differences (42–90 kPa) when measured at a distance of 75 mm^2. Reducing the size of reactants enhances the reactivity of pyrotechnics by enlarging the interfacial contact areas between reactants[10]. Apart from the excellent combustion performance of nanothermites, Selvakumar[11] also found that nanoscale flash powder ($Al/S/KNO_3$) with a higher completeness of reaction consumes only 25 wt% of the microscale powder needed to emit the same noise level. The effect of loading density on the combustion propagation of nanothermites has been studied by researchers. As reported by Ahn[12], with increasing density of the Al/CuO nanothermite, the unconfined burn rate decreases rapidly at low pellet densities (38–52% theoretical maximum density (TMD)) and decreases gradually at high pellet densities (52–80% TMD), while the pressurization characteristics decrease obviously. However, there are few reports on the effects of loading density, confinement strength, and initiation mode on pyrotechnics.

To evaluate the destructiveness of explosion scenes and the inverse calculation of charge mass, the reactivities of the applied explosive materials must be considered as the basis. In practical cases, criminals can obtain industrially manufactured pyrotechnics by disassembling commercial fireworks and crackers, and producing unknown or little-studied hazardous materials by randomly mixing oxidizers and fuels for application in illegal scenarios. Moreover, criminals may intend to increase lethality by loading more explosive materials into their containers, in other words, increasing the loading density. Therefore, finding out the reactivities of unauthorized explosive materials under different conditions is vital for facilitating the investigation and analysis of explosion scenes. In this paper, we explore the reactivities of unstudied binary pyrotechnics consisting of powerful fuels of aluminum microparticles and nanoparticles and three of the most common oxidizers potassium nitrate, potassium chlorate, and ammonium perchlorate under various loading densities. These results can provide useful information for the field of forensic science, such as IEDs disposal, damage evaluation, accident analysis, inverse calculations of explosive source parameters, and personal protection.

Experimental section

Materials

Aluminum nanoparticles (nAl, ~50 nm) and microparticles (mAl, ~1 μm) are purchased from HAOXI Research Nanomaterials (Shanghai), Inc. The active content of Al is approximately 74.2 wt% as measured by thermogravimetric analysis (TG) under air purge. Potassium nitrate (KNO_3), potassium chlorate ($KClO_3$), ammonium perchlorate (NH_4ClO_4, or AP), and n-hexane are supplied by Sinopharm chemical reagent Co., Ltd.

Pyrotechnic preparation

To minimize the agglomeration of solid particles, the binary pyrotechnics are mixed in an ultrasonic bath. In general, Al and oxidizers are added to n-hexane, and then the suspensions are sonicated for 60 min using an ultrasonic cleaner (KQ-300DB, Kunshan Ultrasonic Instruments Co., LTD). Finally, the uniformly dispersed suspensions are poured onto a dish to remove solvent in a fume hood. Due to the existence of alumina shell on the surface of Al powders, the optimum mass ratios of the reactants are determined by their pressurization characteristics, as shown in Fig. S1 and Table 1. The equivalence ratio (φ) of Al/oxides is defined as Eqs. (1)–(4),

$$\varphi = \frac{(F/O)_a}{(F/O)_s} \tag{1}$$

where $(F/O)_s$ is the stoichiometric ratio of Al/oxides as described by Eqs. (2), (3), and (4), $(F/O)_a$ is the actual ratio of Al/oxides. The morphologies of the prepared pyrotechnics are captured by a field-emission scanning electron microscope (SEM), while the dispersion of constituents is qualitatively evaluated by an attached energy dispersive spectrometer (EDS).

$$10Al + 6KNO_3 \rightarrow 3Al_2O_3 + 5K_2O + 3N_2\,(g) \tag{2}$$

Samples	φ	Mass ratio	Loading density (g cm^{-3})	Mass of loaded powders (mg)
Al/KNO_3	1.4	38.4/61.6	1.0, 1.25, 1.50, 1.75, 2.0, 2.20	114, 143, 171, 200, 229, 252
$Al/KClO_3$	1.4	34.6/65.4	1.0, 1.25, 1.38, 1.50, 1.75	114, 143, 158, 171, 200
Al/NH_4ClO_4	2.0	43.4/56.6	1.0, 1.25, 1.38, 1.50, 1.75	114, 143, 158, 171, 200

Table 1. Details of the prepared pyrotechnics.

$$2KClO_3 + 4Al \rightarrow 2KCl + 2Al_2O_3 \quad (3)$$

$$6NH_4ClO_4 + 10Al \rightarrow 4Al_2O_3 + 3N_2\,(g) + 12H_2O\,(g) + 2AlCl_3 \quad (4)$$

Thermal analysis

The thermodynamics of the samples at low heating rate are measured using a thermogravimetry/differential scanning calorimetry (TG-DSC) instrument (STA 6000, PerkinElmer). Approximately 1 mg of samples are placed in an alumina crucible under argon flow and heated from room temperature to an end temperature of 800 °C at a heating rate of 10 K/min.

Measurement of pressurization characteristics

To obtain the optimum ratio of Al/oxidizers, the pressurization characteristics of pyrotechnics are measured using a combustion cell with ~15 mL volume equipped with a piezoelectric pressure sensor (CY–YD–205, Sinocera Piezotronics, INC) coupled to a charge amplifier (YE5854A, Sinocera Piezotronics, INC). For a typical test, 25 mg of samples consisting of nAl or mAl particles are placed on a bowl-like combustion base, as shown in Fig. 1a, and ignited by a nichrome (Ni–Cr) wire with a diameter of 0.2 mm, which is in direct contact with the samples. Time-resolved pressure curves are recorded by an oscilloscope. The Maximum pressure and pressurization rate are then extracted to evaluate the reactivity of the samples. To compare the pressurization characteristics of pyrotechnics loaded at various densities, a cylindrical combustion base, as shown in Fig. 1b, with an inner diameter of 3 mm is used.

Prediction of adiabatic combustion performance

The effect of loading density on the combustion performance of these binary explosives is theoretically predicted using the NASA–CEA thermochemical codes[13] with UV (constant volume) option. For the calculations, the density of the pyrotechnics ranges from 0.25 to 2.2 g cm^{-3}, and the size of reactants is not considered. Based on the minimization-of-free-energy formulation, details output performance for given mixtures can be predicted, including adiabatic flame temperature (T_v), the species, mole fraction and thermodynamic state of products, average molar mass of products (M), and so on. Additional, impetus (f_v) can be obtained by Eq. (8), which is a key parameter to evaluate the working capability of energetic materials,

$$f_v = nRT_v \quad (5)$$

where n and R are the mole number of gaseous products and universal gas constant, respectively. For a given volume (V) and mass (m), the impetus of samples is proportional to produced pressure (P), and can be calculated by Eq. (9) based on the ideal gas state equation.

$$f_v = \frac{P \cdot V}{m} \quad (6)$$

Visual combustion propagation recording

The prepared pyrotechnics are loaded into open-ended transparent quartz tubes, which allow visual recording by a high-speed camera (CP70-2-M/C-1000, Optronis), as shown in Fig. 2. The inner and outer diameters of the quartz tubes are 3 mm and 9 mm, respectively. The powders are poured into a tube, which is placed in a charging mould, and then compressed into pellets using a lever press. The length of loaded samples is set as 10 mm, hence the mass varies by loading density (Table 1). The pellets are then ignited by a Ni–Cr heating wire. The exposure time and aperture of the high-speed camera are set to 10 μs and F8.0, respectively. All tests are carried out in ambient air.

Results

Morphological characterization

Figure 3 displays SEM images of the raw materials and composites. Solid oxidizer particles with uniform sizes are obtained via a solvent–antisolvent recrystallization method (distilled water–ethanol for KNO_3 and $KClO_3$, and *N*–*N* dimethylformamide–dichloromethane for AP). The dimensions of the refined KNO_3, $KClO_3$, and AP particles are 7.13 μm×3.24 μm, 2.35 μm×1.83 μm, and 2.49 μm×1.87 μm, respectively. The components of the prepared pyrotechnics are uniformly dispersed without obvious agglomeration. For example, aluminum

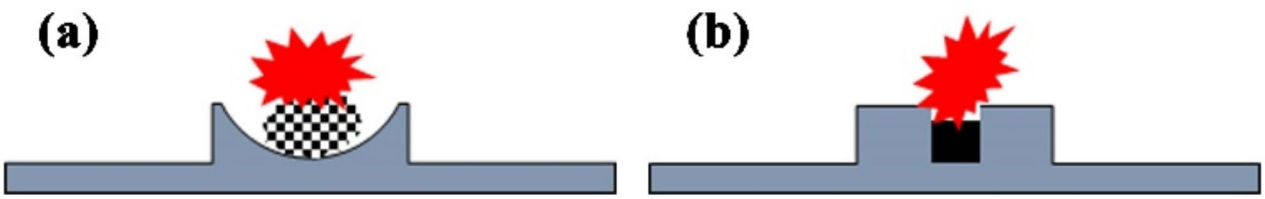

Fig. 1. Schematic of (**a**) bowl-like combustion base and (**b**) cylindrical combustion chamber used in pressurization characteristics tests.

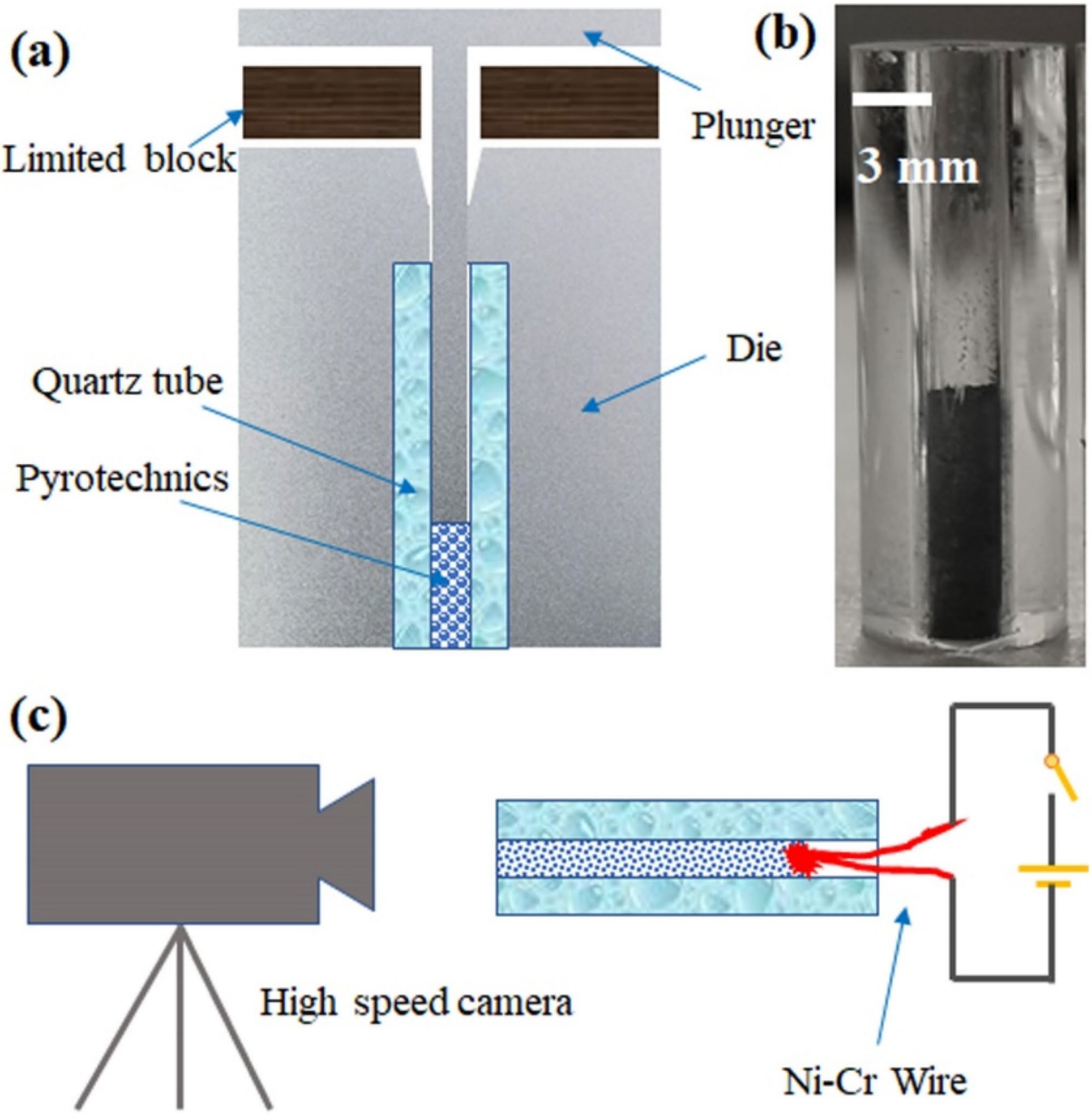

Fig. 2. Experiment setup used for visual combustion propagation recording: (**a**) charging mold, (**b**) a quartz tube loaded with pyrotechnics, and (**c**) recording setup.

nanoparticles (nAl) are spread over the surfaces of KNO_3 microparticles, as shown in Fig. 3e. In contrast, relatively few Al microparticles (mAl) rest on the surfaces of $KClO_3$ particles (Fig. 3g) due to their similar diameters, resulting in a relatively small contact area. The EDS mapping analysis of mAl/$KClO_3$ (Fig. 3h) confirms that the compositions are dispersed uniformly, as clearly indicated by the element maps of potassium (K) (green), chloride (Cl) (blue) and Al (red), which are attributed to the $KClO_3$ and nAl components of the mixture.

Thermodynamic results

Table 2; Fig. 4, and Fig. S2 present the thermal analysis results of the prepared pyrotechnics, revealing that the addition of Al particles alters the thermodynamics of the oxidizers. For the pure refined KNO_3, there are three main endothermic peaks corresponding to phase conversion (135 °C), melting (329 °C), and thermal decomposition (679 °C)[14]. After mixing, one exothermic peak occurs in the range of 475 to 650 °C due to the gas–solid reaction occurring between Al and the KNO_3 decomposition products. There is an endothermic peak (352 °C) of melting and an exothermic peak (520 °C) of decomposition[15] in the DSC curve of the refined $KClO_3$.

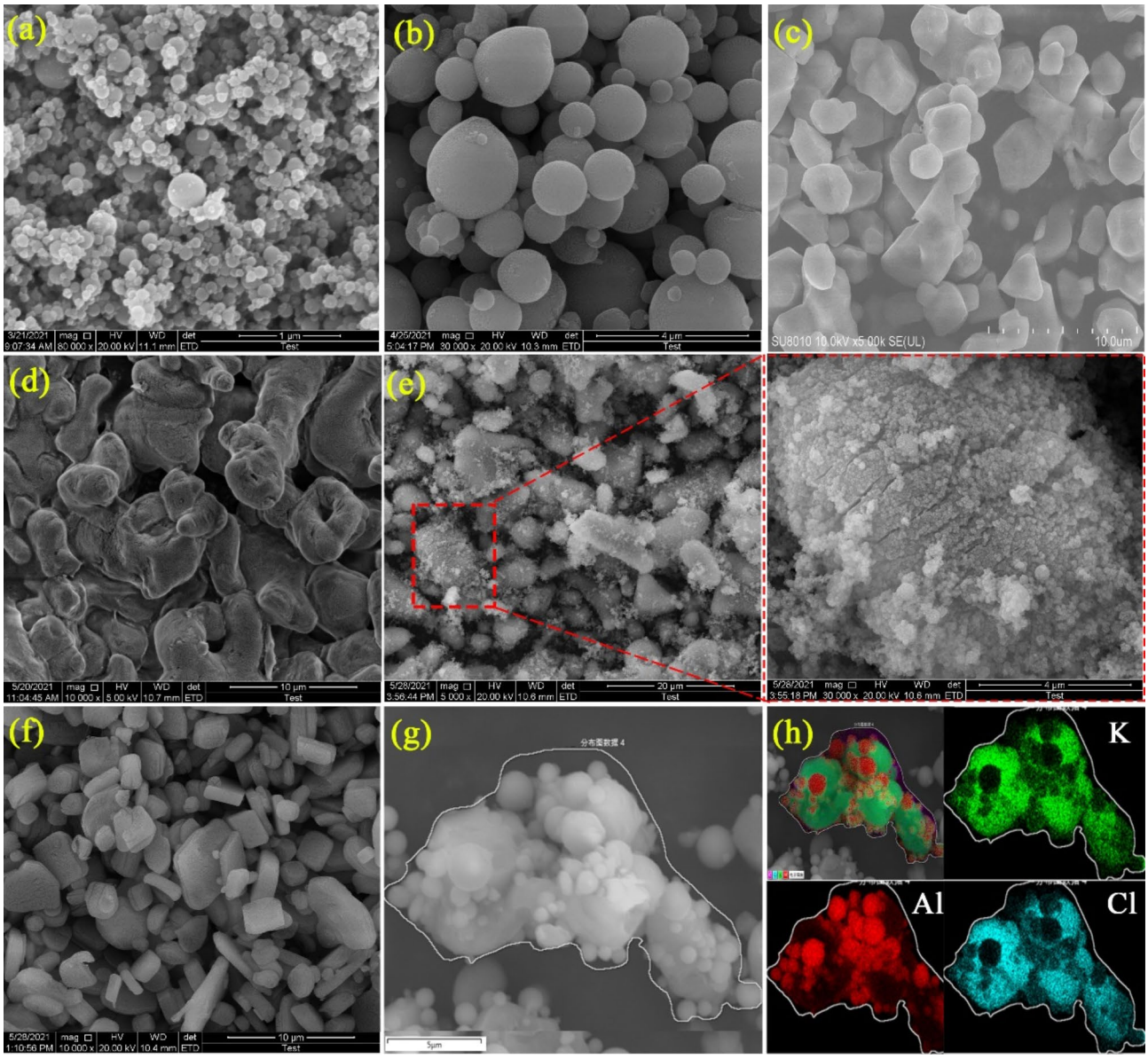

Fig. 3. SEM images of (**a**) nAl, (**b**) mAl, (**c**) refined AP, (**d**) refined KNO_3, (**e**) nAl/KNO_3 with enlarged zone, (**f**) refined $KClO_3$, (**g**) mAl/$KClO_3$, and (**h**) elemental maps for K, Al, Cl (K = green, Al = red, and Cl = blue) of mAl/$KClO_3$.

Samples	Theoretical mass loss	Mass loss without thermite reaction	Mass loss TG results	Temperature of exothermic peak (°C)	Heat release (J g^{-1})
KNO_3	53.5%	–	64.4%		
nAl/KNO_3	9.6%	33.0%	13.5%	555	1895.2
mAl/KNO_3	9.6%	33.0%	28.1%	600	768.8
$KClO_3$	39.2%	–	31.1%		
nAl/$KClO_3$	0	25.6%	13.9%	552	2197.0
mAl/$KClO_3$	0	25.6%	18.9%	599	599.4
AP	100%	–	95.7%		
nAl/AP	30.8%	56.6%	50.5%	577	2222.0
mAl/AP	30.8%	56.6%	62.9%	608	2039

Table 2. Thermal analysis results of the oxidizers and the prepared pyrotechnics.

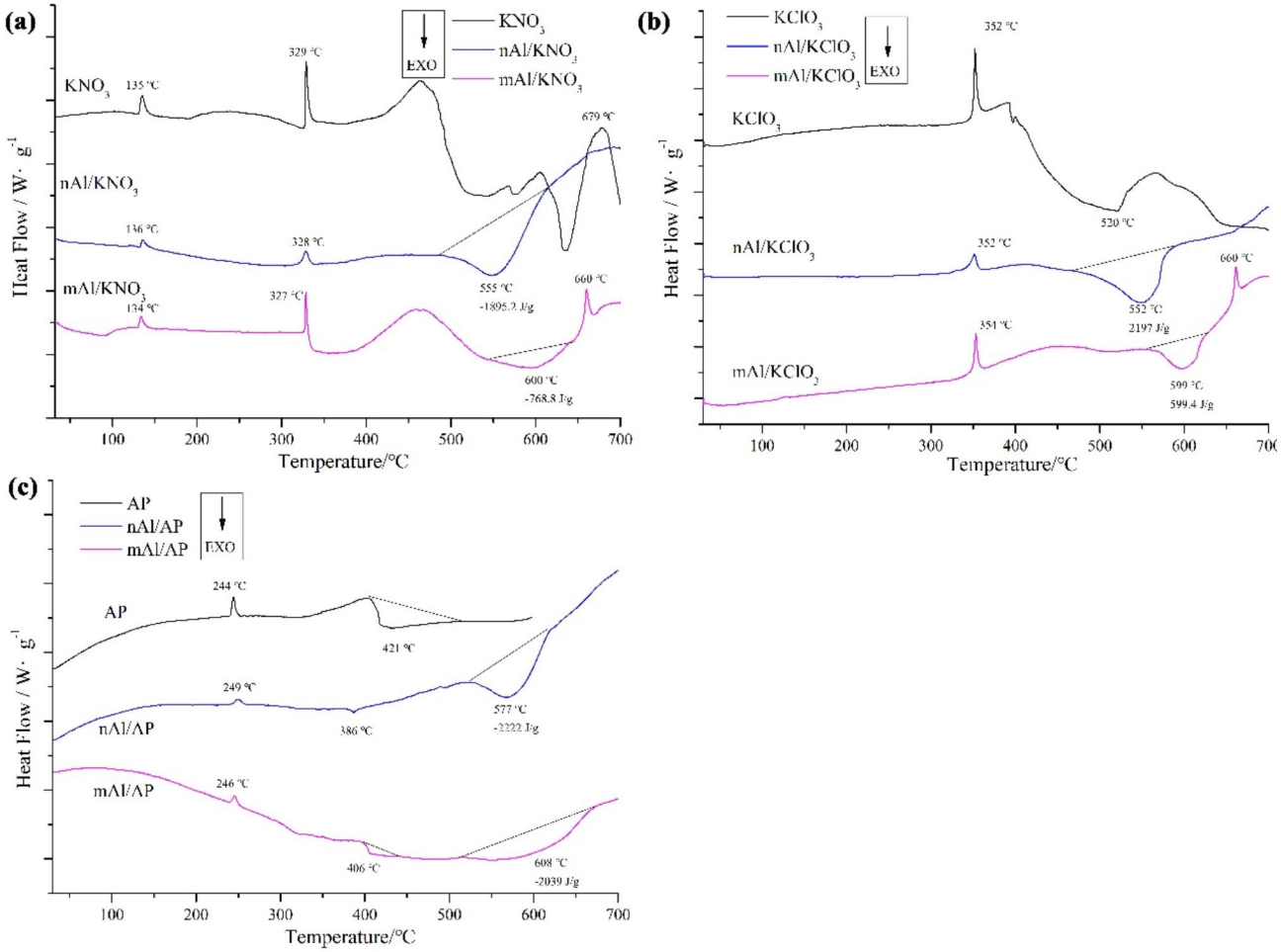

Fig. 4. DSC curves of the refined oxidizers and the prepared pyrotechnics.

In the mixture of Al/$KClO_3$, the exothermic peak on account of the thermite reaction shifts to a relatively high temperature. The decomposition of the refined AP mainly consists of an endothermic peak (244 °C) of phase transition and an exothermic peak of high-temperature decomposition (HTD)[16]. The addition of Al particles shifts the HTD stage to a lower relatively low temperature, while the thermite reaction between AP and Al also occurs below the melting point of Al (660 °C).

The results also reveal that the nAl-based pyrotechnics possess excellent reactivity with a relatively low exothermic peak temperature, a relatively high amount of released heat, and a high completeness level of the reaction. During heating, an obvious weight loss of the pure refined oxidizers caused by the runaway of gaseous decomposition products can be observed. Al reacts with the decomposition products in a manner of gas–solid reaction, releasing substantial heat. The exothermic peak temperature of nAl/KNO_3 is 45 °C lower than that of mAl/KNO_3, while the amount of heat released is nearly 2.5 times greater (1895.2 vs. 768.8 J g^{-1}). Similar differences exist in the other two systems. As summarized in Table 2, the theoretical weight losses of pyrotechnics described by Eqs. (2), (3) and (4) are 9.6%, 0%, and 30.8%, respectively. The theoretical weight losses of pure KNO_3, $KClO_3$, and AP in the prepared mixture should be 33%, 26.6%, and 56.6%, respectively, as expressed by Eqs. (5), (6), (7)[14–16], specifically, only the decomposition of the oxidizer should be considered without undergoing further thermit reaction.

$$4KNO_3 \rightarrow 2K_2O + 2N_2\,(g) + 5O_2\,(g) \tag{7}$$

$$2KClO_3 \rightarrow 2KCl + 3O_2\,(g) \tag{8}$$

$$2NH_4ClO_4 \rightarrow 2O_2\,(g) + N_2\,(g) + 4H_2O\,(g) + Cl_2\,(g) \tag{9}$$

However, the measured weight losses of the prepared pyrotechnics are between the theoretical values of these pyrotechnics and the theoretical weight losses of pure oxidizers, except for mAl/AP. For example, the TG result of nAl/KNO_3 is 13.5%, and the corresponding theoretical values of the pyrotechnic itself and pure KNO_3 are 9.6% and 33.0%, respectively. This finding suggests that partially decomposed gaseous products escape without the occurrence of thermit reaction. The high mass loss of the mAl-based pyrotechnics indicates that more gaseous decomposition products escape with relatively low completeness of the reaction and the presence of superfluous

mAl. These results can be verified by the endothermic peak of Al melting (~ 660 °C) in mAl/KNO_3 and mAl/$KClO_3$. Similar phenomena can be observed for Al/$KClO_3$ and Al/AP.

Seemingly, the diameters of the Al particles have the most significant effects on the $KClO_3$-based pyrotechnics, as the amount of heat released from mAl/$KClO_3$ (2197.0 J g^{-1}) is much lower than that of nAl/$KClO_3$ (599.4 J g^{-1}), and combustion propagates more slowly than that of mAl/AP. The decomposition processes of both $KClO_3$ (370–600 °C) and AP (400–500 °C) release heat, rather than absorb heat. This may be one factor explaining why the KNO_3-based pyrotechnics have the lowest pressurization levels. Compared to KNO_3 and $KClO_3$, AP reacts with Al more completely, as no endothermic peak appears after the thermit reaction, and the reaction is more powerful as the amount of heat released is relatively high, especially in the case of mAl/AP, resulting in a high combustion propagation velocity.

Pressurization characteristics of pyrotechnics

Table 3 presents a summary of the pressurization characteristics of the prepared pyrotechnics combust on a bowl-like combustion base. The mixture of mAl and KNO_3 cannot combust completely even with the aid of Al/Fe_2O_3 nanothermite which is one high energy priming, therefore, no data are available. Compared to the other two systems, the $KClO_3$-based pyrotechnics exhibit the best pressurization characteristics. For example, the pressurization rate (dp/dt) of nAl/$KClO_3$ (7.58 MPa ms^{-1}) is one order of magnitude higher than that of both nAl/KNO_3 (0.37 MPa ms^{-1}) and nAl/AP (0.94 MPa ms^{-1}), and the combustion duration (t_c) is the shortest (0.38 ms). When Al nanoparticles are replaced by microparticles, mAl/$KClO_3$ reacts more intensely than mAl/AP, with a higher dp/dt (0.064 vs. 0.028 MPa ms^{-1}) and shorter t_c (2.97 vs. 13.24 ms). The mixtures with nAl obviously exhibit superior pressurization characteristics to those of the mAl-based pyrotechnics. Compared to those of mAl/$KClO_3$ and mAl/AP, the dp/dt of nAl-based pyrotechnics is approximately1 ~ 2 orders of magnitude greater (7.58 vs.0.064, and 0.94 vs. 0.028 MPa ms^{-1}, respectively), and the peak pressure (P_{max}) is more than two times greater (1.37 vs.0.43, and 1.22 vs. 0.54 MPa, respectively); correspondingly, the t_c is one order of magnitude lower (0.38 vs.2.97, and 0.88 vs.13.24 ms, respectively). Nanoparticles have a smaller diameter and greater surface area than microparticles; hence, the distances between Al and the oxides are shorter for nAl-based pyrotechnics than for mAl-based pyrotechnics, thereby increasing the heat and mass transfer efficiencies between fuels and oxides and intensities of reactions. Similar to the change in thermodynamic behavior, the pressurization characteristics of Al/$KClO_3$ attenuate more sharply than those of Al/AP when mAl replaces nAl.

Predicted reactivities of pyrotechnics at various loading densities

The calculation results are shown in Fig. 5 and Fig. S3. With increasing density, the total mole fraction of main condensed products for Al/KNO_3 or Al/$KClO_3$ increases monotonically, but the change in Al/AP is negligible. The average molar mass of products (M) in Al/KNO_3 or Al/AP increases persistently while that of Al/$KClO_3$ shows a contrary tendency. As a comprehensive result of the change in mole fraction of condensed products and M, the gaseous products mole number for Al/KNO_3 or Al/AP decrease monotonically going against violent combustion, but it decreases firstly and then slightly rises for Al/$KClO_3$. Meanwhile, the predicted values of T increase monotonically, thereinto, the increment for Al/$KClO_3$ is the largest. These results indicate that the loading density can alter the reaction process of the pyrotechnics. As the product of n and T, the produced P of Al/KNO_3 or Al/AP per unit mass decreases steadily with increasing density. The variation tendencies are consistent with the measured values. The calculated values of the impetus of Al/$KClO_3$ loaded at the range of density from 0.75 to 2.20 g cm^{-3} exhibit a general increase. However, the overmuch predicted values of T (7000–9000 K) may be the reason why the variation tendency of the experiment values is opposite as the produced P scales with the released heat and the moles of gaseous products.

Pressurization characteristics of pyrotechnics at various loading densities

The pressure cell results for pyrotechnics loaded at various densities are summarized in Fig. 6 and Fig. S4. Due to the low reactivity and high heat loss in a cylindrical combustion chamber, the pellets of mAl/$KClO_3$ cannot combust in a self-sustaining manner; therefore, no data are available. In addition to the open combustion space of the bowl-like combustion base, the semi-confined combustion environment provided by the cylindrical combustion chamber enhances the reaction completeness of pyrotechnics, but may hinder the diffusion of gaseous products, resulting in different pressurization characteristics. The results show that the loading density has different effects on the variations in the pressurization behaviors of the three systems. The pressurization process of nAl/KNO_3 is obviously affected by the loading conditions, and an abrupt decrease in the reactivity occurs in the density range of 1.0 to 1.25 g cm^{-3}. When nAl/KNO_3 is loosely loaded (1.0 g cm^{-3}), the dp/dt and P_{max} of nAl/KNO_3 are 0.175 MPa ms^{-1} and 0.96 MPa, respectively. When the powders are slightly compressed (1.25 g cm^{-3}), dp/dt decreases by one order of magnitude to 0.024 MPa ms^{-1}, P_{max} decreases by approximately

Samples	P_{max} (MPa)	dp/dt (MPa ms^{-1})	Combustion durations (ms)
nAl/KNO_3	0.81 ± 0.067	0.37 ± 0.035	2.04 ± 0.38
nAl/$KClO_3$	1.37 ± 0.048	7.58 ± 0.32	0.38 ± 0.034
mAl/$KClO_3$	0.43 ± 0.013	0.064 ± 0.010	2.97 ± 0.14
nAl/NH_4ClO_4	1.22 ± 0.099	0.94 ± 0.086	0.88 ± 0.12
mAl/NH_4ClO_4	0.54 ± 0.024	0.028 ± 0.002	13.24 ± 0.39

Table 3. Pressurization characteristics of the prepared pyrotechnics.

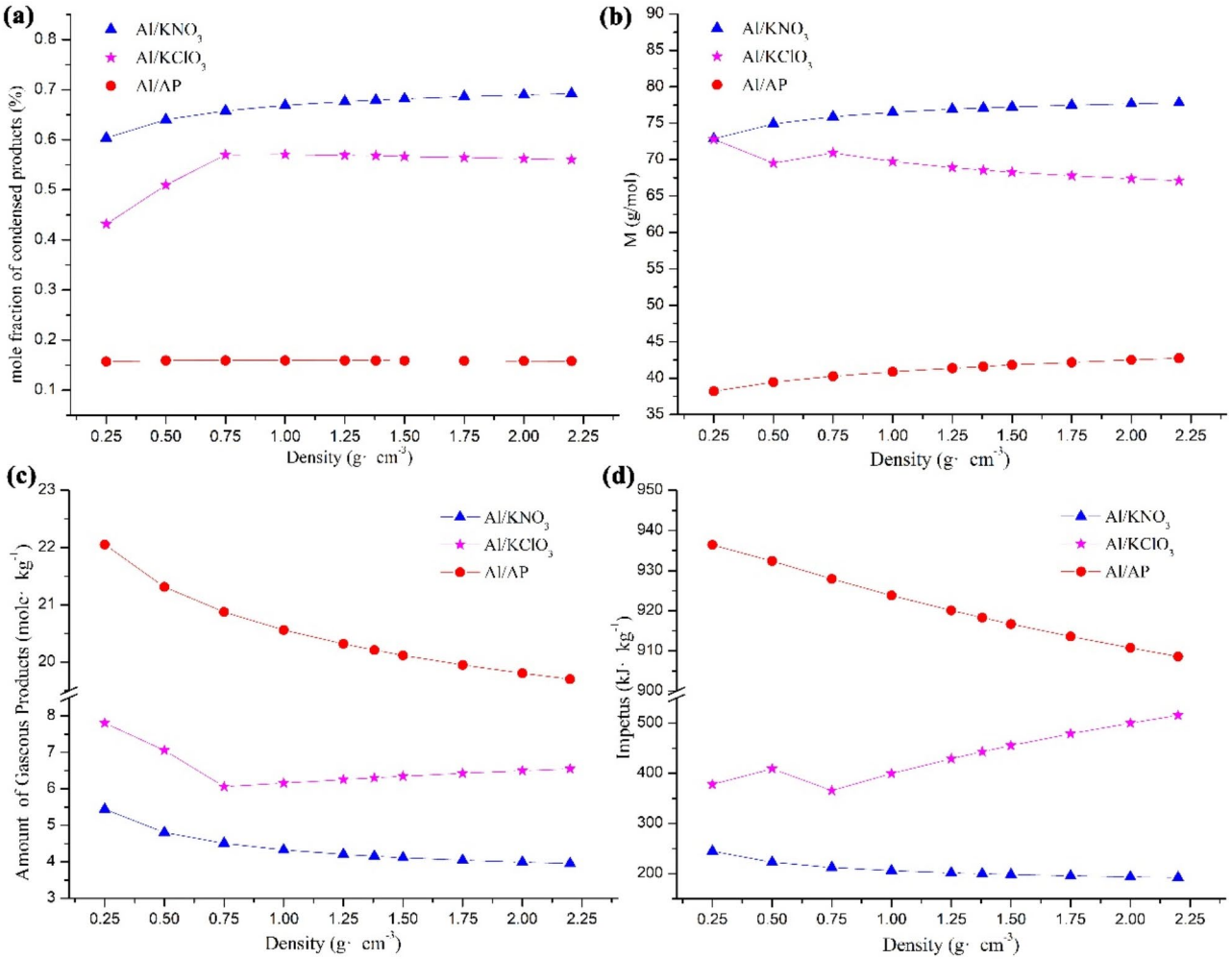

Fig. 5. Predictions using NASA–CEA for the constant volume combustion of the pyrotechnics: (**a**) mole fraction of main condensed products, (**b**) average molar mass of products, (**c**) amount of gaseous products (n) and (**d**) impetus (f_v) at various densities.

half to 0.50 MPa, and t_c increases from 0.49 ms to 14.6 ms. With increasing loading density, the pressurization characteristics further decrease slightly to 0.35 MPa, 0.014 MPa ms^{-1}, and 16.7 ms. Loading conditions seem to mildly impact the reactivity of nAl/$KClO_3$. In the density range of 1.0–1.75 g cm^{-3}, the dp/dt and t_c values fluctuate around 30 MPa ms^{-1} and 0.35 ms, respectively, while the P_{max} decreases by 17%. This result indicates that nAl/$KClO_3$ can maintain superior reactivity even when loaded at a high density. For nAl/AP, the abrupt decline in the pressurization characteristics occurs at a density of 1.50 g cm^{-3}, at which point six trials are conducted. When the loading density increases from 1.0 g cm^{-3} to 1.38 g cm^{-3}, the values of dp/dt and P_{max} decrease gradually. When the loading density reaches 1.50 g cm^{-3}, distinct pressurization behaviors (3 trials of rapid reaction and 3 trials of slow reaction) are observed. For rapid reaction, the values of the pressurization characteristics are 1.94 MPa, 0.38 MPa ms^{-1}, and 2.18 ms, respectively. In contrast, these values of the slow reaction decrease greatly to 0.50 MPa, 0.027 MPa ms^{-1}, and 11.0 ms, respectively. With increasing loading density of mAl/AP, the values of dp/dt and P_{max} decrease linearly by 62% and 89%, respectively. No available pressure-time curve of mAl/AP is obtained when the loading density exceeds 1.38 g cm^{-3}.

Besides the size of reactants, loading conditions also have a significant impact on the efficiency of heat and mass transfer during reaction propagation. Increasing loading density facilitates conductive heat transfer, but goes against convective heat transfer and accompanied mass exchange, leading to a decreasing reactivity with low gaseous products yield, as proven by the decreasing pressurization characteristics of mAl/AP. For pyrotechnics composed of nanoparticles, increasing loading density over a certain range would induce an abrupt transition of dominant heat transfer mode from convective to conductive, resulting in an abrupt transition of reactivity as shown in the case of nAl/KNO_3 and nAl/AP. The certain range of loading density strongly depends on the intrinsic characteristics of reactants. Due to the superior yield of gaseous products, the transition density range of nAl/AP (~ 1.50 g cm^{-3}) is higher than that of Al/KNO_3 (between 1.0 and 1.25 g cm^{-3}). For nAl/AP, the dp/dt values differ by orders of magnitude with a loading density of 1.50 g cm^{-3}, suggesting that the dominant heat transfer mode was oscillating between convective and conductive at this point. Besides, the relatively small

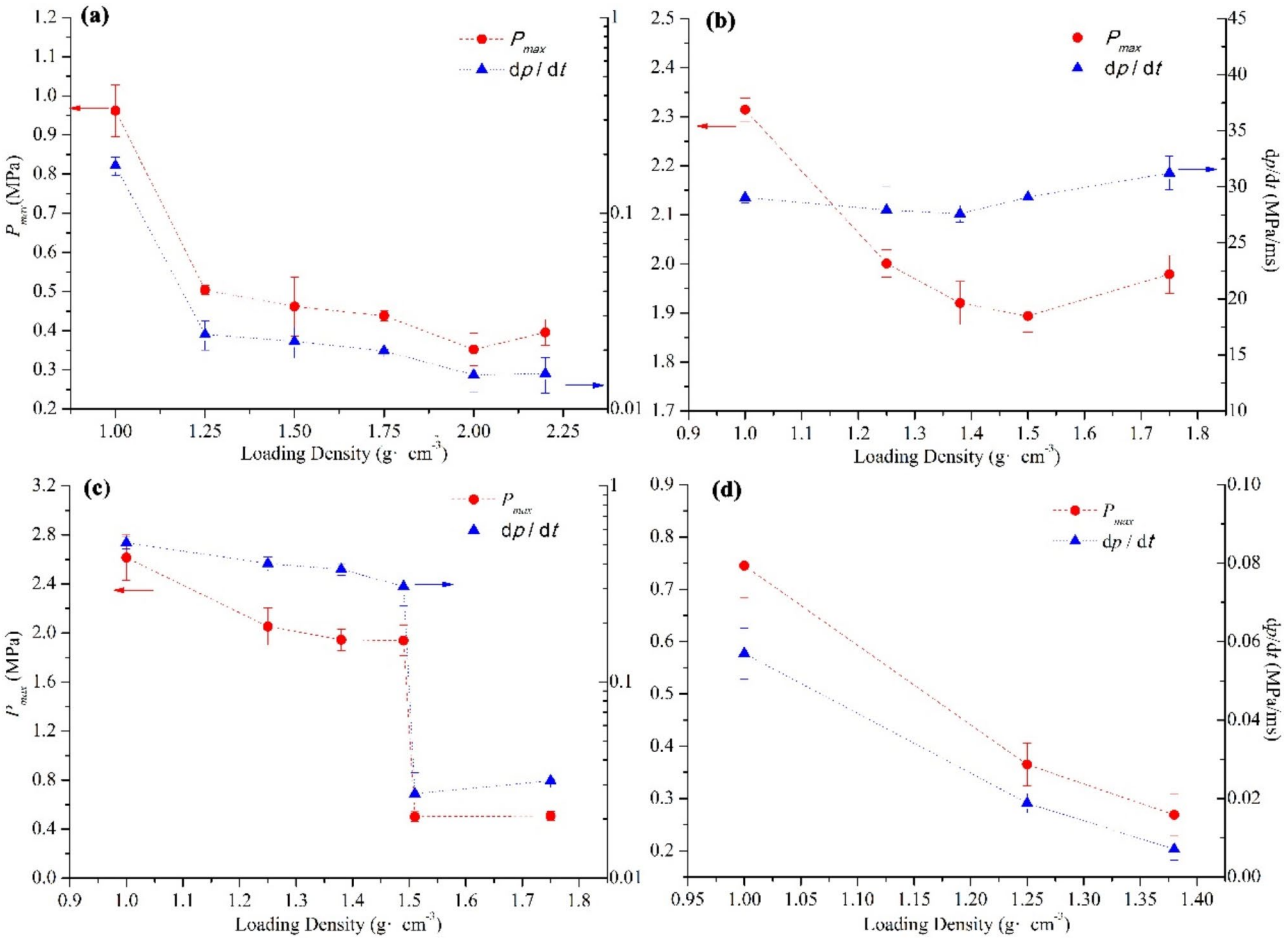

Fig. 6. Pressurization characteristics of (**a**) nAl/KNO_3, (**b**) nAl/$KClO_3$, (**c**) nAl/AP and (**d**) mAl/AP loaded at various densities.

mass of loaded powders (~ 25 mg) may lead to a great error for loading density, resulting in distinct output performances. In previous reports, similar phenomena were also observed. For example, an abrupt transition of thrust forces and burn durations was observed at 52.5% TMD for Al/Bi_2O_3/NC(2.5%)[17], and the reaction-regime transition occurred at 44.4% TMD for Al/CuO nanothermite[18]. In addition of its low ignition temperature confirmed by DSC results, Al/$KClO_3$ could maintain quite high pressure output at high loading density as predicted by CEA codes making the variation tendency of pressurization of nAl/$KClO_3$ is not clear.

Combustion propagation behaviors

The combustion propagation processes of pyrotechnics loaded at various loading densities are recorded by a high-speed camera. Quartz tubes filled with nAl//$KClO_3$ or nAl/AP are easily shattered even at a high loading density due to the rapid expansion of gaseous products within several milliseconds; thus, no data are available. As shown in Fig. 7, the combustion propagation processes of nAl/KNO_3 vary at different loading densities. The combustion front propagates from the up to the down, and the dotted line (yellow) represents the upper boundary of the quartz tube. The dashed straight lines (red) that connect combustion fronts indicate that these combustions propagate at a constant speed. The combustion of loosely loaded (1.0 g cm^{-3}) nAl//KNO_3 is intense with a sharply shaped flame front, and the propagation duration is only 240 μs. Flames inside the tube are luminous because of the high mass flux of hot products. The nAl//KNO_3 loaded at a density of 1.5 g cm^{-3} combusts in the manner of end-burning with a steady front, and the propagation duration reaches to 194 ms.

The combustion behaviors of mAl//$KClO_3$ at various loading densities change obviously as shown in Fig. 8a and b. When the loading density is 1.0 g cm^{-3}, the front propagation duration is 0.44 s with a brighter flame inside the tube, while it is 1.3 s at 1.5 g cm^{-3}. As the loading density increases, combustion propagates relatively slowly with decreasing the mass flux of the products, and more condensed state products remain on the inner wall (Fig. 8c) leading to a darker flame that can be observed inside the tube.

The positions of the flame front as a function of time in each test are first extracted by ImageJ software and then fitted by linear fitting, as shown in Fig. S5. The combustion propagation speed (v_p) is the value of the slope of the fitted line. Figure 9 displays the v_p values of nAl/KNO_3, mAl/$KClO_3$, and mAl/AP at various loading densities. The combustion behaviors of nAl/KNO_3 obviously change the most significantly. The v_p decreases sharply by three orders of magnitude from 48.8 ± 18.6 m s^{-1} to 0.045 ± 0.008 m s^{-1} as the loading density increases from

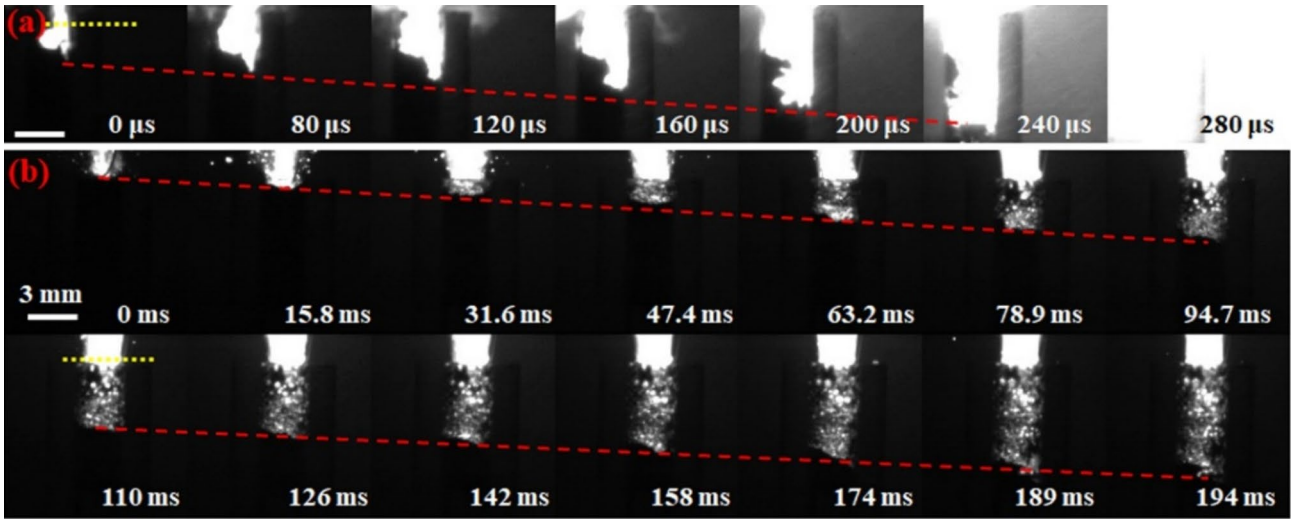

Fig. 7. Combustion of nAl/KNO_3 loaded at (**a**) 1.0 g cm^{-3} and (**b**) 1.5 g cm^{-3}.

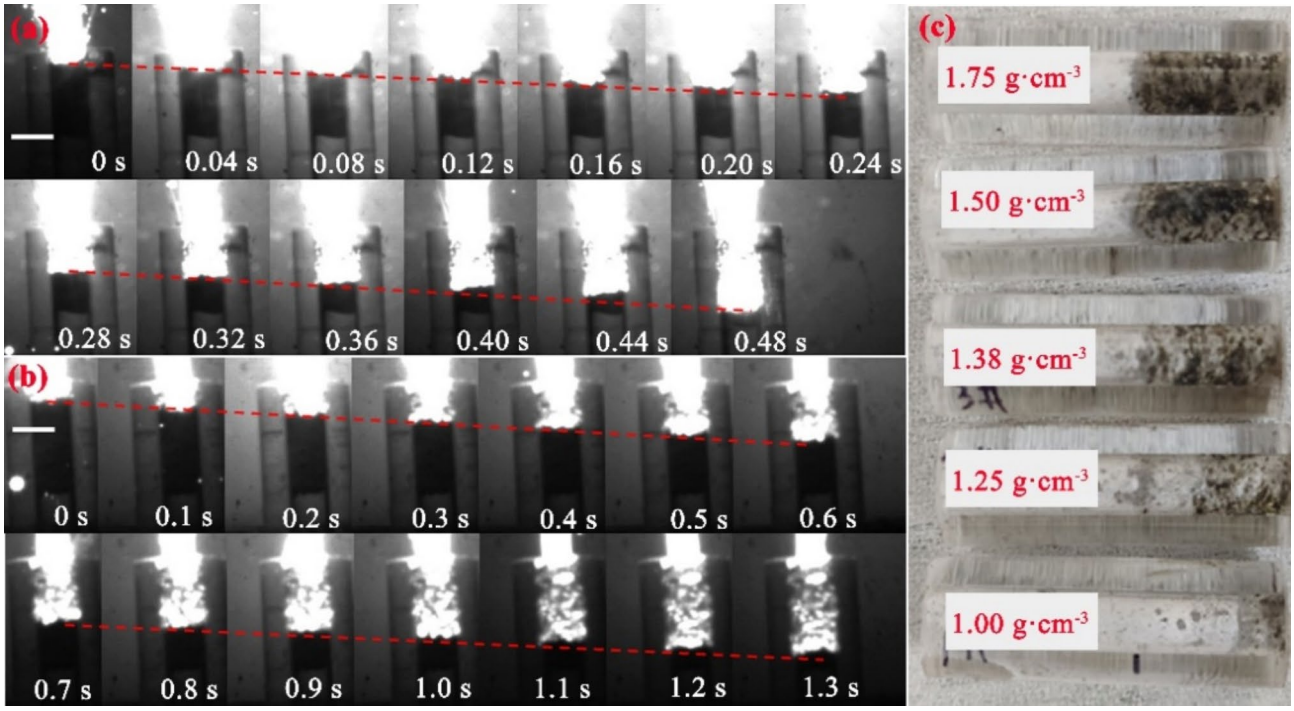

Fig. 8. Combustion of mAl/$KClO_3$ loaded at (**a**) 1.0 g cm^{-3} and (**b**) 1.5 g cm^{-3}, and (**c**) combustion residues of mAl/$KClO_3$ on the inner wall of quartz tubes.

1.0 g cm^{-3} to 1.25 g cm^{-3}. With the continuous increase in the loading density (1.50 g cm^{-3} to 2.20 g cm^{-3}), v_p slightly increases from 0.040 m s^{-1} to 0.078 m s^{-1}. The v_p of mAl/AP decreases linearly by one order of magnitude from 1.36 ± 0.38 m s^{-1} (1.0 g cm^{-3}) to 0.31 ± 0.13 m s^{-1} (1.25 g cm^{-3}) and then to 0.10 ± 0.06 m s^{-1} (1.38 g cm^{-3}). The combustion of mAl/$KClO_3$ propagates mildly with the lowest v_p, which decreases gradually from 16.7 ± 5.8 mm s^{-1} to 4.6 ± 0.4 mm s^{-1} as the loading density increases from 1.0 g cm^{-3} to 1.75 g cm^{-3}.

Discussion

For a typical pyrotechnics-based IED, the base charge can be ignited by a hot wire excited by a power source or a fuse, which then reacts in a self-sustaining manner of combustion or deflagration, producing abundant hot gaseous and condensed products. When the internal pressure of the container resulting from the expansion of hot gaseous products exceeds its strength, an explosion occurs, as shown in Fig. 10. The intensity of the explosion is closely related to the reactivity of the applied charge. In addition to reaction kinetics based on

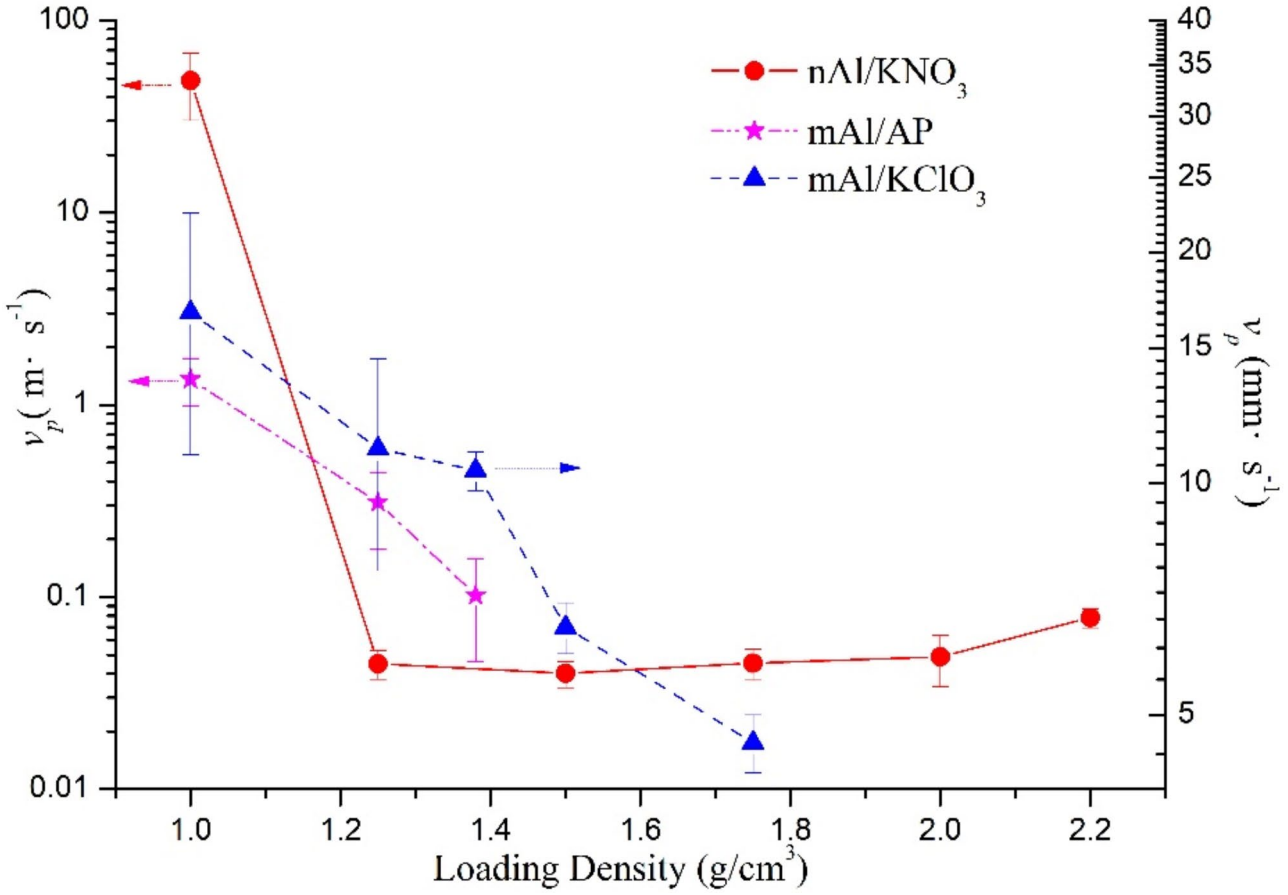

Fig. 9. Combustion front propagation velocities of nAl/KNO_3, mAl/$KClO_3$, and mAl/AP loaded at various loading densities.

the inherent nature of energetic materials, the reactivities of pyrotechnics are governed by the mass and heat transfer efficiencies, i.e. heat transfer in the form of conduction, convection, and radiation, and the movements of hot substances involving condensed and gaseous products between the combusted region and unreacted region. Among these behaviors, convective heat transfer and the exchange of accompanying materials (gaseous and condensed products) exchange are the main contributors to the maintenance of high-speed combustion propagation[19–21].

According to Darcy's law, the porosity of loaded materials and the pressure gradient directly affect the propagation behaviors of fluids. When pyrotechnics are loaded into a container, voids between particles, which serve as channels for concomitant substance transport, spread across the grain. Under a low loading density, the presence of numerous sufficient voids between particles guarantees that convection is the dominant mode of heat transfer facilitating high-speed combustion propagation and superior pressurization characteristics. For example, convection dominates at a loading density of 1.0 g cm^{-3} for nAl/KNO_3 and at a loading density below 1.5 g cm^{-3} for nAl/AP; for the KNO_3-based pyrotechnics, the loading density at which convection dominates is not clear.

Increasing the loading density decreases the porosity of grains, which is favorable for enhancing the thermal conductivities of loaded materials by enlarging the contact areas of solid particles for one thing[22]. This is an explanation that why the v_p of nAl/KNO_3 increases slightly when its loading density exceeds 1.5 g cm^{-3}. Conversely, increasing the loading density can close a certain number of channels for convective heat transfer and for mass transport[23]. The contribution of heat conduction to sustaining a high combustion propagation speed is fairly low, even estimated by upper bound[20], while the decrease in the convective heat transfer efficiency is exponential. Hence, when the loading density increases above a specific value, conduction becomes the dominant heat transfer mode with a relatively low combustion propagation velocity (i.e., conduction dominates at current densities of 1.25 g cm^{-3} for nAl/KNO_3 and 1.5 g cm^{-3} for nAl/AP). A relatively high gaseous product is also beneficial for convective heat transfer and concomitant substance transport due to a great pressure gradient. Therefore, the maximum loading density corresponding to the high-level reactivity of either nAl/AP or nAl/$KClO_3$ with a high peak pressure is greater than that of nAl/KNO_3.

Notably, the combustion ambient pressure significantly affects the mass and heat transfer efficiencies of pyrotechnics. As reported by Weismiller[24], increasing the ambient pressure changes the dominant propagation mechanism of heat transfer from convective to conductive, thereby drastically decreasing the combustion

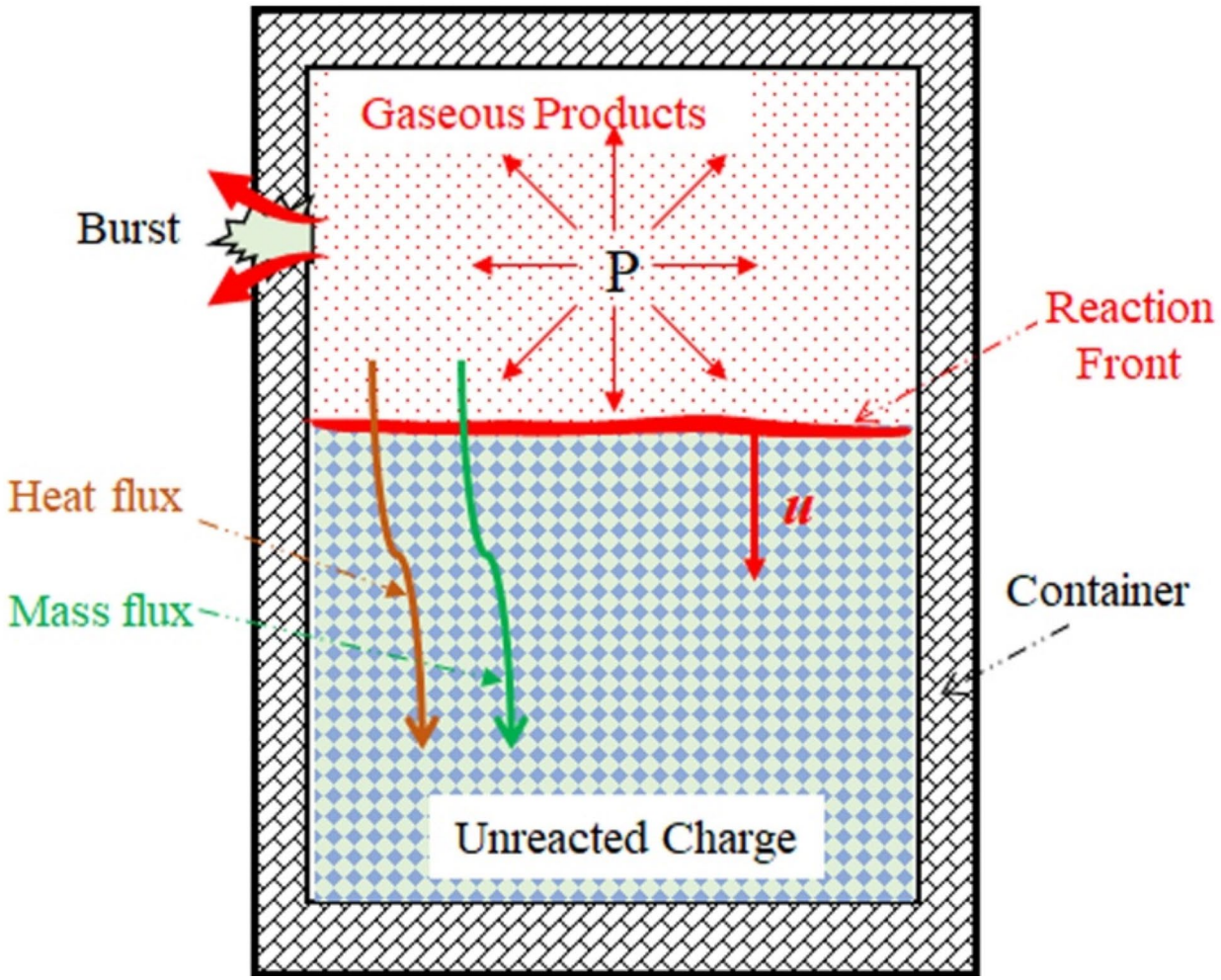

Fig. 10. Schematic of combustion propagation of pyrotechnics in a closed container.

velocity of Al/CuO nanothermite from ~1000 m s^{-1} to ~1 m s^{-1}. This phenomenon is completely different from that of propellants or explosives. Therefore, increasing the loading density of pyrotechnics in IEDs can reduce the fluxes of gaseous products, and take a relatively long time to build pressure within an enclosed space; furthermore, the buildup pressure can further degrade combustion propagation, weakening the destructive power of the explosion.

Conclusion

In the field of forensic science, a comprehensive understanding of the properties of explosive materials used in IEDs is critical for investigating and analyzing explosion scenes. With the increasing difficultly in the acquisition of standard explosives and initiators, pyrotechnics are becoming a common explosive source of IEDs. In this paper, the reactivities of homemade binary pyrotechnics, which are sensitive to the reactant species and operating conditions, are systematically studied to improve the accuracy of evaluations of explosion damage and inverse calculations of charge parameters. The morphologies, thermodynamics, pressurization characteristics and combustion propagation behaviors of the samples are characterized. Compared with the participation of KNO_3 or AP, the participation of $KClO_3$ promotes pyrotechnics release more gaseous products, especially in the case of nAl/$KClO_3$, within a relatively short time. The dp/dt of nAl/$KClO_3$ (7.58 MPa s^{-1}) is an order of magnitude greater than that of the others, while the dp/dt of mAl/$KClO_3$ (0.062 MPa s^{-1}) is more than twice of mAl/AP. The diameter of Al has an obvious impact on the thermodynamics and pressurization characteristics of the pyrotechnics as expected. A small particle size leads to an increasingly intimate contact between the reactants, which shortens the heat and mass transfer distance. As a result, the nAl-based pyrotechnics have a relatively low exothermic reaction peak temperature and high amount of released heat, implying that intense reactions occur. When mAl replaces nAl, mAl/KNO_3 cannot combust in a self-sustaing manner, and the P_{max} and dp/dt values of the other two systems decrease by more than half and by orders of magnitude, respectively. As predicted by the NASA–CEA thermochemical codes, varying loading density would alter the amount of gaseous products and adiabatic flame temperature of the pyrotechnics, leading to a decrease in the produced pressure per unit mass for Al/KNO_3 or Al/AP, and an increase for Al/$KClO_3$. Changing the loading density alters the internal microstructure of the applied charge and directly affects the heat and mass transfer efficiencies. Increasing the

loading density decreases the number of channels available for heat convection and the accompanying exchange of products, and changes the dominant modes of heat and mass transfer. For nAl/KNO_3, a sharp decrease in the reactivity appears between 1.0 and 1.25 g cm^{-3}, across which dp/dt decreases by one order of magnitude, and v_p decreases by three orders of magnitude. Distinct pressurization behaviors of nAl/AP are observed at 1.5 g cm^{-3}; however, the variation in the reactivity of nAl/$KClO_3$ is chaotic. The consequence of the weakened reactivity is that the accumulation of pressure inside the IED containers is slowed. Furthermore, the explosion output of pyrotechnics prepared under various conditions including lethality, shock wave strength, fragment morphology, residues identification, etc., should be explored to construct a database for forensic science.

Data availability

All the data are available on request from the corresponding author.

Received: 30 May 2024; Accepted: 6 November 2024
Published online: 11 November 2024

References

1. Kunz, S. N., Zinka, B., Peschel, O. & Fieseler, S. Accidental head explosion: An unusual blast wave injury as a result of self-made fireworks. *Forensic Sci. Int.* **210**, 4–6 (2011).
2. Weitzel, W. R. *Evaluation of Overpressure Wave Transition by Airblast Overpressure And Shock Wave Attenuation Analysis Using a Small Black Powder Charge*. Master thesis, University of Kentucky (2014).
3. Verma, S. K. Homicide by improvised explosive device made out of firecrackers. *Med. Sci. Law*. **41**, 353–355 (2001).
4. Zelkowicz, A., Tenne, D., Kirshenbaum, Y. K., Rossin, A. & Mishraki-Berkowitz, T. A method for Rapid separation of perchlorate and Nitrate Salts in pyrotechnic and improvised explosive mixtures. *J. Forensic Identif.* **70**, 231–244 (2020).
5. Bors, D., Cummins, J. & Goodpaster, J. The anatomy of a pipe bomb explosion: The effect of explosive filler, container material and ambient temperature on device fragmentation. *Forensic Sci. Int.* **234**, 95–102 (2014).
6. Kirschman, J., Pokutta-Paskaleva, A., Courtney, A. & Courtney, M. Blast pressures and waveforms of consumer firecrackers. *Shock Waves*. **31**, 301–306 (2021).
7. Otłowski, T., Zalas, M. & Gierczyk, B. Forensic analytical aspects of homemade explosives containing grocery powders and hydrogen peroxide. *Sci. Rep.* **14**, 750 (2024).
8. Vermeij, E., Duvalois, W., Webb, R. & Koeberg, M. Morphology and composition of pyrotechnic residues formed at different levels of confinement. *Forensic Sci. Int.* **186**, 68–74 (2009).
9. Zwirner, J. et al. Suicide by the intraoral blast of firecrackers: Experimental simulation using a skull simulant model. *Int. J. Legal Med.* **131**, 1581–1587 (2017).
10. Junghare, S., Kumari, S., Chaudhary, A., Kumar, R. & Rayalu, S. Thermite reaction driven pyrotechnic formulation with promising functional performance and reduced emissions. *J. Hazard. Mater.* **424**, 127345 (2022).
11. Selvakumar, N., Azhagurajan, A. & Suresh, A. Experimental analysis on nano scale flash powder composition in fireworks manufacturing. *J. Therm. Anal. Calorim.* **113**, 615–621 (2013).
12. Ahn, J. Y. et al. Combustion characteristics of high-energy Al/CuO composite powders: The role of oxidizer structure and pellet density. *Powder Technol.* **241**, 67–73 (2013).
13. Gordon, S. & Mcbride, B. J. *Computer Program for Calculation of Complex Chemical Equilibrium Compositions and Applications. Part 1: Analysis* (NASA Lewis Research Center, 1994).
14. Hosseini, S. G. & Eslami, A. Thermoanalytical investigation of relative reactivity of some nitrate oxidants in tin-fueled pyrotechnic systems. *J. Therm. Anal. Calorim.* **101**, 1111–1119 (2010).
15. Ravanbod, M., Pouretedal, H. R., Amini, M. K. & Ebadpour, R. Kinetic study of the thermal decomposition of potassium chlorate using the non-isothermal TG/DSC technique. *Cent. Eur. J. Energ. Mater.* **13**, 505–525 (2016).
16. Deng, P., Wang, H., Yang, X., Ren, H. & Jiao, Q. Thermal decomposition and combustion performance of high-energy ammonium perchlorate-based molecular perovskite. *J. Alloys Compd.* **827**, 154257 (2020).
17. Staley, C. S. et al. Fast-impulse nanothermite solid-propellant miniaturized thrusters. *J. Propul Power*. **29**, 1400–1409 (2014).
18. Apperson, S. J. et al. Characterization of nanothermite material for solid-fuel microthruster applications. *J. Propul Power*. **25**, 1086–1091 (2009).
19. Egan, G. C. & Zachariah, M. R. Commentary on the heat transfer mechanisms controlling propagation in nanothermites. *Combust. Flame*. **162**, 2959–2961 (2015).
20. Kline, D. J. et al. Experimental observation of the heat transfer mechanisms that drive propagation in additively manufactured energetic materials. *Combust. Flame*. **215**, 417–424 (2020).
21. Wu, T. et al. Engineered porosity-induced burn rate enhancement in dense Al/CuO nanothermites. *ACS Appl. Energy Mater.* **5**, 3189–3198 (2022).
22. Stacy, S. C., Zhang, X., Pantoya, M. & Weeks, B. The effects of density on thermal conductivity and absorption coefficient for consolidated aluminum nanoparticles. *Int. J. Heat Mass Transf.* **73**, 595–599 (2014).
23. Kagan, L. & Sivashinsky, G. Theory of the transition from conductive to convective burning. *Proc. Combust. Inst.* **33**, 1983–1988 (2011).
24. Weismiller, M. R., Malchi, J. Y., Yetter, R. A. & Foley, T. J. Dependence of flame propagation on pressure and pressurizing gas for an Al/CuO nanoscale thermite. *Proc. Combust. Inst.* **32**, 1895–1903 (2009).

Acknowledgements

This work was supported by the Science and Technology Planning Project of Ministry of Public Security (2022JC05), the Natural Science Foundation of Liaoning Province (2023MS134), the National Natural Science Foundation of China (21805310), the Fundamental Research Funds for the Central Universities (3242019019), the Key Laboratory of Forensic Science Open Project of Liaoning Province (FTKX2022KF01), Young Backbone Teachers Scientific Research Funding Project of Shenyang Institute of Technology (QN202205).

Author contributions

The manuscript was prepared through the contributions of all authors. All authors have given approval to the final version of the manuscript. C.R.: Conceptualization and design of study, Data analysis and interpretation, Original draft writing and editing; L.C.: Methodology, Morphological characterization; H.Z.: Samples preparation, Thermal analysis; H.W.: Pressurization characteristics measurements; H.X.: Theoretical calculations; Z.C.:

Combustion propagation measurements; Y.Z.: Draft review and editing, Supervision.

Declarations

Competing interests
The authors declare no competing interests.

Additional information
Supplementary Information The online version contains supplementary material available at https://doi.org/10.1038/s41598-024-79212-6.

Correspondence and requests for materials should be addressed to Y.Z.

Reprints and permissions information is available at www.nature.com/reprints.

Publisher's note Springer Nature remains neutral with regard to jurisdictional claims in published maps and institutional affiliations.